MERCI: Mixed curvature-based elements for computing equilibria of thin elastic ribbons: supplementary information

RAPHAËL CHARRONDIÈRE, Univ. Grenoble Alpes, Inria, CNRS, Grenoble INP, LJK, France
SÉBASTIEN NEUKIRCH, Sorbonne Université, CNRS, Institut Jean Le Rond d'Alembert, UMR 7190, France
FLORENCE BERTAILS-DESCOUBES, Univ. Grenoble Alpes, Inria, CNRS, Grenoble INP, LJK, France

CCS Concepts: • **Computing methodologies** → **Animation**; **Physical simulation**.

Additional Key Words and Phrases: Thin elastic ribbon, curvature-based element, constraints, contact, Möbius band

ACM Reference Format:
Raphaël Charrondière, Sébastien Neukirch, and Florence Bertails-Descoubes. 2024. MERCI: Mixed curvature-based elements for computing equilibria of thin elastic ribbons: supplementary information. 1, 1 (May 2024), 4 pages. https://doi.org/XXXXXXX.XXXXXXX

1 INTRODUCTION

We gather here some additional computations and information.

2 MÖBIUS IN ONE SHOT

If the point $s = 0$ is set at the singular point, we show in the LUA-interface script in the supplementary files that the simple seed (aka warmstart) configuration

$$\kappa_{\text{seed}}(s) = 2\,\pi \tag{1}$$

$$\eta_{\text{seed}}(s) = \cos\left(2\,\pi\,s\right) \tag{2}$$

is enough for Merci to converge within 30 Ipopt iterations to the Möbius solution in less than two seconds (100 segments, $w/L = 0.1$), see Figure 1.

3 MÖBIUS WITH SINGULAR REGION IN THE MIDDLE

In the main text, we pointed out that the singular point (where $w\,\eta' = \pm 2$) is difficult to go through in shooting-based models. Consequently, many numerical approaches use setups where the singular point of the Möbius solution is at an edge of the integration interval. In this section, we place the singular point in the middle of the integration interval and show that Merci does not suffer from the same drawback. Moreover, we demonstrate

Authors' addresses: Raphaël Charrondière, Univ. Grenoble Alpes, Inria, CNRS, Grenoble INP, LJK, 38000, Grenoble, France, raphael.charrondiere@inria.fr; Sébastien Neukirch, Sorbonne Université, CNRS, Institut Jean Le Rond d'Alembert, UMR 7190, 4 place Jussieu, case 162, F-75005, Paris, France, sebastien.neukirch@upmc.fr; Florence Bertails-Descoubes, Univ. Grenoble Alpes, Inria, CNRS, Grenoble INP, LJK, 38000, Grenoble, France, florence.descoubes@inria.fr.

XXXX-XXXX/2024/5-ART $15.00
https://doi.org/XXXXXXX.XXXXXXX

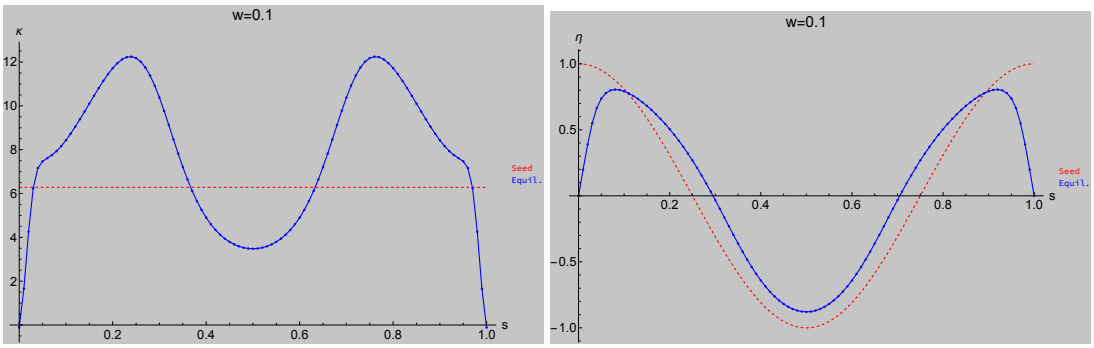

Fig. 1. Möbius solution (blue) and seed (red) with the singular point at the edge of the s interval. Left: solution for $\kappa(s)$. Right: solution for $\eta(s)$. With 100 elements, the minimisation requires 30 IPOPT iterations and takes less than 2 seconds to converge.

the ease of use of MERCI by showing that only a rough estimate of the solution for $\kappa(s)$ and $\eta(s)$is sufficient to obtain convergence. We warm-start the minimisation procedure with

$$\kappa_{\text{seed}}(s) = -2\,\pi\,\tanh\left(c\,[s-1/2]\right) \tag{3}$$

$$\eta_{\text{seed}}(s) = \tanh\left(c\,[s-1/2]\right)\,\cos\left(2\,\pi\,s\right) \tag{4}$$

and obtain the solution after a few dozen IPOPT iterations, see the LUA-interface script in the supplementary files. We show in Figure 2 the functions $\kappa_{\text{seed}}(s)$, $\eta_{\text{seed}}(s)$ together with the equilibrium solutions $\kappa(s)$ and $\eta(s)$. We

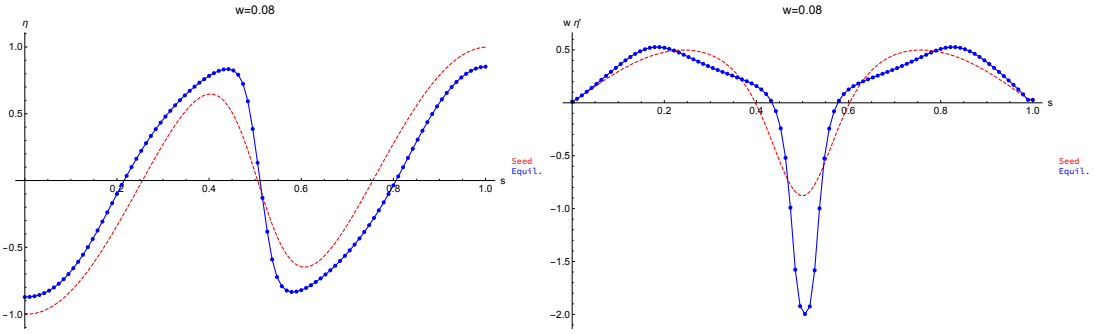

Fig. 2. Möbius solution (blue) and seed (red, with $c = 11$ and $w/L = 0.08$) with the singular point in the middle of the integration interval. Left: solution for $\kappa(s)$. Right: solution for $\eta(s)$. With 95 elements, the minimisation requires 70 IPOPT iterations and takes less than 3 seconds to converge.

show in Figure 3 the shape of the equilibrium solution with the singular point clearly visible.

4 APPROXIMATION OF THE HEIGHT OF THE PLANAR ELASTICA

The value $H_0(\Delta)$ is computed from the planar elastica solution [Bigoni 2012; Love 1944]

$$\frac{H_0(\Delta)}{L} = \frac{\sqrt{m}}{K(m)} \tag{5}$$

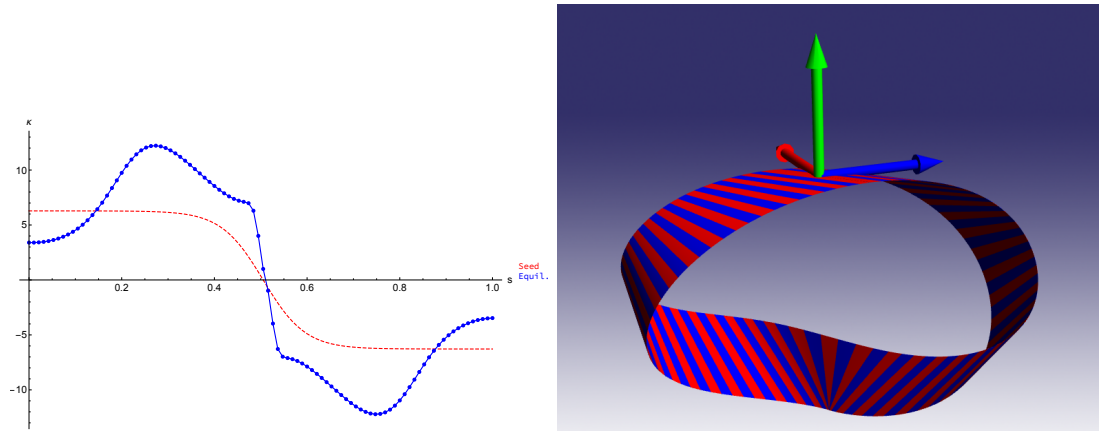

Fig. 3. Möbius solution ($w/L = 0.08$) showing the material frame at $s = 0$, and the rapidly varying rule orientation near the singular point at $s = 1/2$.

where $K(m) = \int_0^{\pi/2} (1 - m \sin^2 \theta)^{-1/2} \, d\theta$ is the complete elliptic integral of the first kind and m is found by numerically inverting

$$\Delta = 2 \left(1 - \frac{E(m)}{K(m)} \right) \tag{6}$$

where $E(m) = \int_0^{\pi/2} (1 - m \sin^2 \theta)^{1/2} \, d\theta$ is the complete elliptic integral of the second kind. In the range $\Delta \leq 0.3$, a good interpolation of $H_0(\Delta)$ is given by

$$\frac{H_0(\Delta)}{L} \simeq \frac{2}{\pi} \sqrt{\Delta} - 0.2 \, \Delta^{1.5}. \tag{7}$$

See also the supplementary Mathematica notebook.

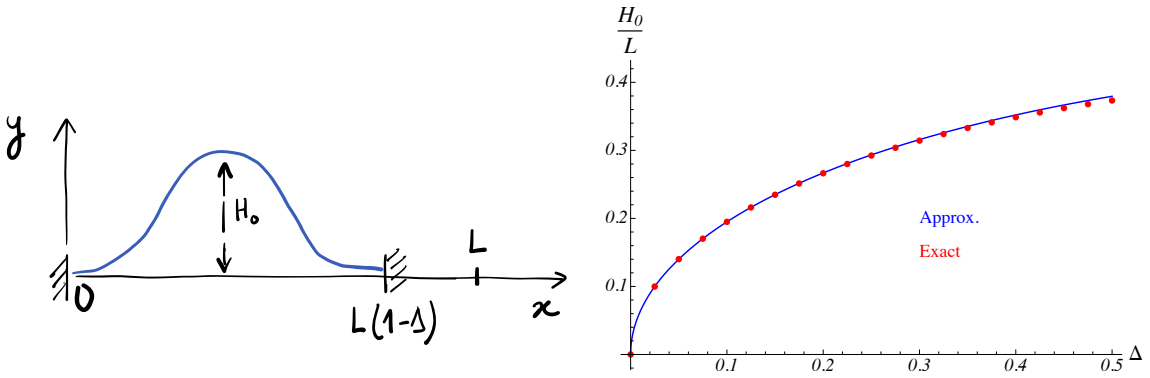

Fig. 4. Height H_0 of the planar elastica as a function of the applied end-shortening Δ. Approximation, given by Eq. 7, and exact value, given by Eq. 5.

5 LATERAL TORSIONAL BUCKLING

To see the influence of the constraint $\eta(0) = 0$, we deactivate it in MERCI and plot the bifurcation curves of the LTB test with the same parameter values as in main the paper, see Figure 5. Note that the buckling thresholds are lower now (for all three Sadowsky, Wunderlich, and Ribext models). On the one hand, MERCI-RIBEXT now buckles exactly at the Kirchhoff threshold, $\Gamma = 18.178(1-\nu)\sqrt{1+\nu}$. Indeed, at this point the function $\boldsymbol{\phi}$ in the Ribext model exactly vanishes, meaning that the Ribext energy matches the Kirchhoff energy for these parameter values. On the other hand, without this constraint $\eta(0) = 0$, we observe a less good agreement between the MERCI-RIBEXT curve and the reference FENICS-SHELL curve.

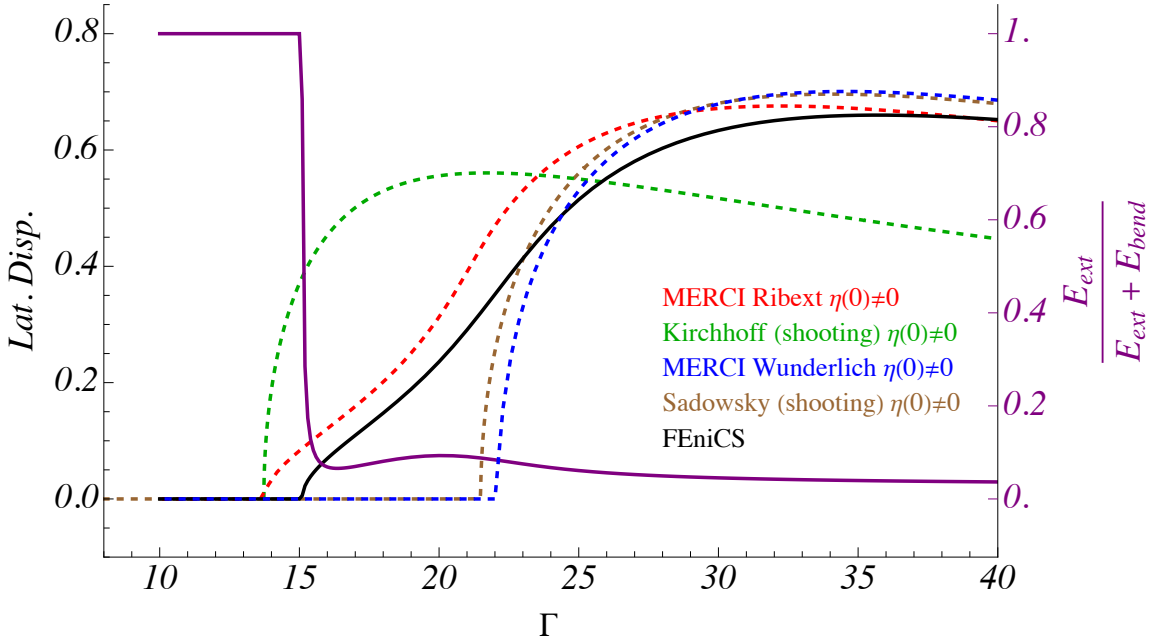

Fig. 5. Lateral Torsional Buckling bifurcation curve with $\nu = 0.35$, $w/L = 0.1$, and $h/L = 0.001$, but without the constraint $\eta(0) = 0$ for the Ribext, Wunderlich, and Sadowsky models.

REFERENCES

Davide Bigoni. 2012. *Nonlinear Solids Mechanics.* Cambridge University Press, Cambridge, UK.
A. E. H. Love. 1944. *A Treatise on the Mathematical Theory of Elasticity* (4th ed.). Dover Publications, New York.